

# **Standardized tensile testing of electro-spun **PA6** membranes via the use of a 3D printed clamping system**

## **Funding Disclosure Statement**

The manuscript has not previously been published in print or electronic form and is not under consideration by any other publication. We declare that there are no ethical problems or conflicts of interest.

## **Abstract:**

This study presents a new design for the jaws used in the uniaxial tensile testing of PA6 electro-spun membranes. The aims of the new design are to both accelerate the clamping process and additionally reduce the paper waste created by paper frames. In order to validate the efficiency of the new design, the newly-developed jaws were compared both with currently-used paper frames and the direct positioning of samples in metal jaws. It was demonstrated that the new jaws reduced the clamping time by half. Moreover, the maximal stress and strain values were observed to be higher than those of the metal jaws and the paper frames. Finally, it was determined that the new design enables the testing of wetted samples, which is problematic using paper frames.

*Keywords:* 3D printed jaws, paper frame, electro-spun membranes, uniaxial tensile test

## Introduction

The use of electro-spun materials is common in many scientific branches due to their wide range of advantageous properties. The production process is simple, inexpensive and allows for the production of ultrafine continuous fibres with a high surface-to-volume ratio and high porosity. Although the electrospinning process has been employed for several years, it has the disadvantage of the need to continuously optimize the spinning conditions so as to adapt to the production of different materials.<sup>1</sup> The tuning and control of the various production parameters are often crucial with respect to advanced biomedical applications such as wound dressings, scaffold engineering approaches, drug delivery devices, medical implants, etc.<sup>2-5</sup> The optimization technology process usually involves the performance of uniaxial tensile tests, which makes up the most fundamental and widely-used approach worldwide. Following an extensive literature review, we can safely state that the uniaxial tensile testing of thin electro-spun membranes is both highly differentiated and, generally, poorly described in the scientific literature. Some authors use the ASTM D882-18 standard method for the testing of the tensile properties of thin plastic sheeting, whereas others do not.<sup>6-11</sup> However, there are two norms that can be applied in case of electro-spun membrane, e.g. ASTM D5035-95 and ASTM D5034-95. Our long-term experience indicates that the scatter in the tensile properties of electro-spun membranes originates both from the nature of the technology used and the systematic character of the testing procedure. The parameter that most influences the speed and the purity of the results comprises the apparatus used for the clamping of electro-spun membranes. While some authors use standardized metal clamps which can cause a fast breakage of the sample close to the clamps. Therefore, an optional inside lining was implemented that aimed at avoiding the breakage of the sample near the clamps<sup>12-14</sup>, others use a paper-based frame for installing samples into the machine clamps<sup>15-20</sup>. The use of the paper frame is convenient. Nevertheless, it indicates an additional preparation of the sample. Alternatively, specialised clamps have been

constructed for this purpose.<sup>21-22</sup>. The list of selected approaches for tensile testing of electro-spun membranes is summarized in Table 1.

**Table 1** List of selected approaches for tensile testing of electro-spun membranes

Authors	Gauge [mm]	Crosshead speed [mm/min]	Clamping system
Yao Ch. et al. 2008	15	10	Metal clamp
Zhao Z. et al. 2005	40	5	Metal clamp
Yano T. et al. 2012	20	10	Not specified
Kumar P. et al. 2017	10	6	Not specified
Tarus B. et al. 2016	40	50	Paper frame
Maksimcuka J. et al. 2017	8	6	Specialised clamps
Elele E. et al. 2019	60	1.6-20%/s	Metal clamp
Feng Y. et al. 2016	20	5	Not specified
D'Amato A. et al. 2018	30	30	Paper frame
Yan J. et al. 2011	20	10	Not specified
Han H. et al. 2020	10	10	Not specified
Xiang Ch. et al. 2016	Not specified	10	Metal clamps
Liu S. et al. 2019	15	5	Metal clamp
Conte A. et al. 2020	10	0.5-50	Plastic frame

Aimed at addressing the shortcomings of the various systems currently available, this study introduces a versatile clamping system that is easy to use and to fabricate. The system builds upon versatile and open source clamps for the tensile testing of soft tissue fabricated by means of 3D printing technology introduced recently for the testing of biological materials.<sup>18,19</sup>

The promising outcomes of this clamping mechanism aims to promise possible standardization of the uniaxial testing, also avoiding the breakage of samples close to the metal clamps, speeding up the process of the sample preparation including the paper frame preparation and gluing the sample into the frame. With the use of the paper frame, the paper waste is connected afterwards the uniaxial test is performed. Moreover, the presented clamping mechanism aims to be used in case of wetted electro-spun membranes.

## Methodology

With respect to low breaking forces, the design of the clamps was based on the ADMET micro tester eXpert 4000 system (Admet Inc, USA). The clamping mechanism was designed using 3D CAD software (Autodesk Inventor, Autodesk, USA) for the testing of electro-spun membranes. The main aims of the design comprised reusability, fast clamping and the avoidance of the sliding of samples during the measurement process. The dimensions of the assembly were designed with respect to the space in the relevant tensile machine and can be scalable to any other type of tensile testing machine. The clamping system itself consist of two identical assemblies (upper and lower). These assemblies are connected by holders needed for easy handling the clamps into the traction machines. The assembly opens via a pin positioned on a side of the jaw. The jaws can be printed on any 3D printer. For increasing the friction between the sample and the clamps and avoiding the sharp edges a silicon block was added into the inner part of the jaw.

For the purposes of 3D printing, it was necessary to export the assembly into universal format stereolithography (.STL). This file was then uploaded into an Objet Connex 500 3D printing machine (Stratasys, USA) that employs PolyJet technology (Stratasys, USA). VeroGray was used as the polymer material (83-86 ShoreD), the chemical composition that was listed by Stratasys is shown in Table 2 with a melting point of 45-50°C. The height of the printing layer was set at 16 µm and the printing time was approximately 5 hours. The silicon parts were produced via vacuum gravitational casting. Therefore, a mould had first to be printed on the same printer, in which the silicon parts were subsequently casted. The silicon material comprised RTV 5510 (Torten s. r. o., Czechia) with a hardness of 10 ShoreA and a hardening time of 8 hours. The silicon parts were then glued to the printed frames.

**Table 2** Chemical composition of VeroGray

Chemical name	Weight-%

Exo-1,7,7-trimethylbicyclo[2.2.1]hept-2-yl acrylate	20-30
Tricyclodecane dimethanol diacrylate	5-10
Titanium dioxide	0.1-1

Reproduced from - <http://www.advancedtek.com/wp-content/uploads/2016/12/SDS-Object-VeroGray-RGD850-US.pdf>

Reproduced from Stratasys Material Sheet

The distribution of contact pressure between the silicon parts was analysed by the finite element (FE) method in the software Comsol Multiphysics® (Comsol Inc., USA). The mesh size was selected according to contact pressure change value lower than 5 % of decrease with the size. The friction between these parts was neglected in the study. The linear elastic material model with defined Young moduli ( $E=0.38$  MPa) and Poisson ratio ( $\nu=0.49$ ) was used in the simulation. The distribution of the contact pressure was the important parameter for the design of the clamping system as it needs to be enough big to hold the sample in a position without slipping during the uniaxial test. Also, the contact pressure should be homogeneously distributed.

An electro-spun membrane produced via polyamide 6 (PA6, Ultramid B27, Basf, Germany) was used as the testing material. The solvent system consisted of acetic and formic acids (Penta Chemicals, Czechia). The PA6 polymer solution was prepared at a concentration of 12 wt% and the ratio of the two acids in the solvent system was 2:1. A magnetic stirrer was used for mixing the solution over a period of 24 hours at room temperature so as to be sure that the polymer was fully dissolved. The prepared solution was electrospun using a Nanospider™ NS 1WS500U (Elmarco, Czechia) with a wire electrode. The voltage was set at 50 kV and the voltage of the opposite collector electrode was -10 kV. The distance between the electrode and the collector was 180 mm. The electrospinning process was conducted at an ambient temperature of 22°C and at a relative humidity of 40%. Electrospinning was performed on a polypropylene base Spunbond fabric. The electrospun membranes were analysed by the

scanning electron microscopy (SEM, Tescan Vega3, Czechia). The membranes were gold plated on Quorum Q150R ES. Afterwards, these samples were placed in Tescan Vega3 (Czechia) and the pictures were taken under a speeded voltage of 20 kV. The scanning electron microscopy samples were further analysed in the software ImageJ for obtaining an average fibre diameter and a fibre distribution.<sup>25</sup>

The design of the system also allowed for the testing of wetted membranes. Therefore, a number of membranes were wetted with a physiological solution (NaCl 0.9%) and subsequently compared to the dry membranes. Three tensile test scenarios were selected for which the strain rate was set at 10 mm/min<sup>26-28</sup>: a standard metal clamp, a paper frame and the new clamp were tested and compared so as to observe their effectiveness and their measurement reproducibility (n=12). Since the jaws were designed for the more rapid clamping of samples, the times required for the placing of samples in the paper frame, including the time required to prepare the paper frame, were compared with the time required for the placing of samples in the printed jaws. Statistical comparison of the data was performed using the TIBCO Statistica™ (Tibco software Inc, USA). The statistical significance of the mean difference of the subgroups was tested using the non-parametric Mann-Whitney test. P-values of 0.05 or less were considered being statistically significant.

## Results and discussion

The 3D CAD model of the novel clamping mechanism used in the uniaxial tensile test is shown in Figure 2A, and a detailed view of the subassembly is shown in Figure 2B. The printed assembly consists of two identical subassemblies with dimensions of 20 x 20 x 10 mm (see Figure 2C), the outer edge of the silicon parts was rounded by a radius of 0.2 mm to avoid the breakage by the edge of the silicon material. The total length of the clamping device was 70 mm including the gauge length of the sample.

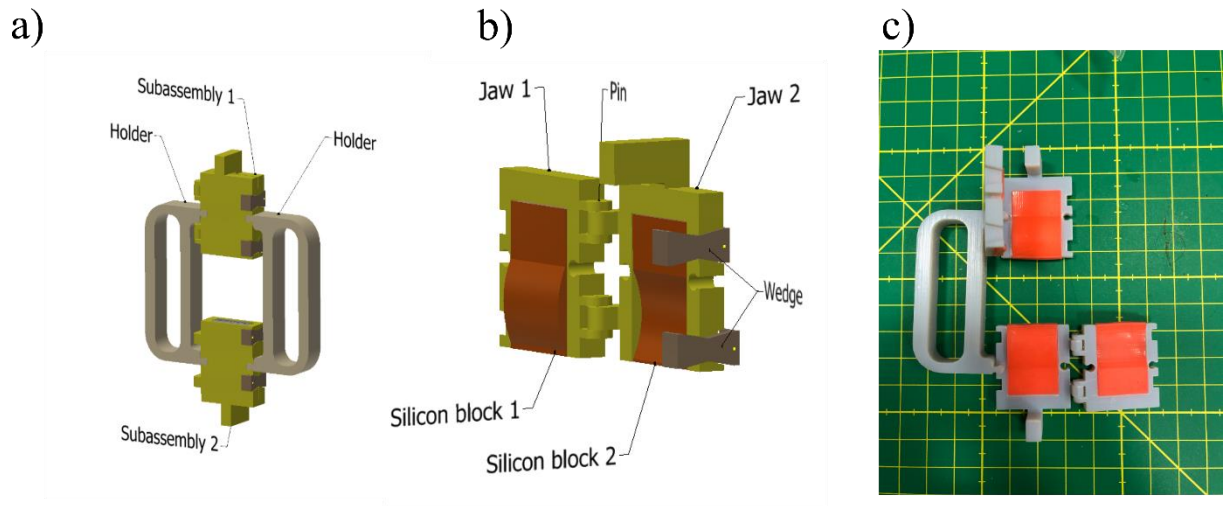


**Figure 1** a) 3D CAD model of the assembly, the subassemblies are closed b) Detailed view of the opened subassembly c) The printed jaws with opened subassemblies

Each of the subassemblies features the jaws that were fabricated via the combination of two materials, i.e. silicon and **VeroGray**. The jaws are connected via two pins and the clamping of the sample is provided for by two wedges that serve to create contact pressure between the silicon components and, thus, ensure the non-sliding of the sample. The length of the sample can be adjusted using a holder which also provides for the easier handling of the sample while it is being positioned in the tensile machine. **The FE results showed homogenous distribution of contact pressure between two silicon parts with no peak contact stress within the contact area, figure 2.**

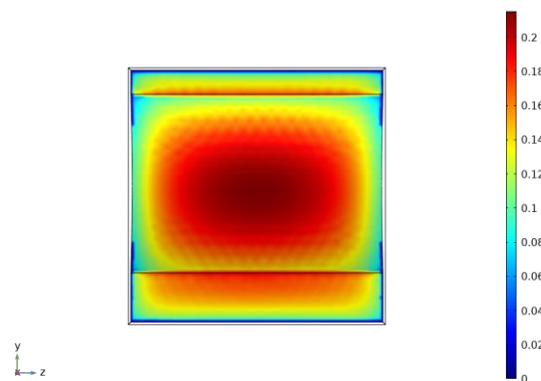


**Figure 2** Distribution of contact pressure within the silicon jaws [MPa]



Figure 3 a shows a sample of dimensions 70x15 mm positioned in the jaws with a gauge length of 30 mm. The used samples had an average fibre diameter of  $0.207 \pm 0.062 \mu\text{m}$  and the distribution of the fibre diameter can be seen in Figure Error! Reference source not found.3c. It was subsequently possible to transfer the sample directly to the tensile machine (see Figure 3b) and the holders were removed.

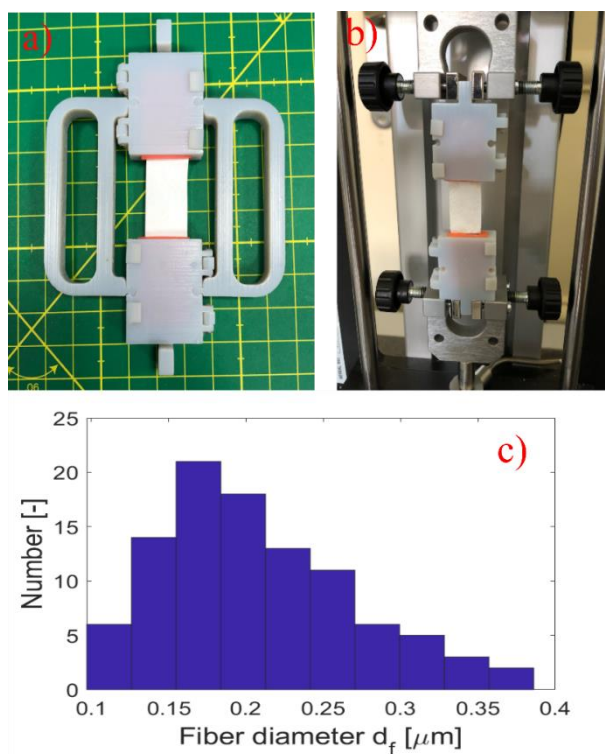


**Figure 3** a) A sample positioned in the jaws, b) A sample positioned in the tensile machine, c) distribution of fibre diameter

The uniaxial tensile test was conducted for the printed jaws and the paper frame, and samples were positioned directly in the metal jaws. The total time required for the preparation and gluing of the paper frame was  $4 \pm 0.5$  minutes per sample whereas direct positioning in the printed jaws took less than 2 minutes ( $90 \pm 15$  seconds), the time of a sample placement was measured starting from the taking of a sample into tweezers and it ended after the holders removal.

**Error! Reference source not found.** illustrates the results of the stress-strain tensile testing of the three approaches to the clamping of the samples. It is evident that the highest strain and stress values were attained using to the 3D printed jaws.

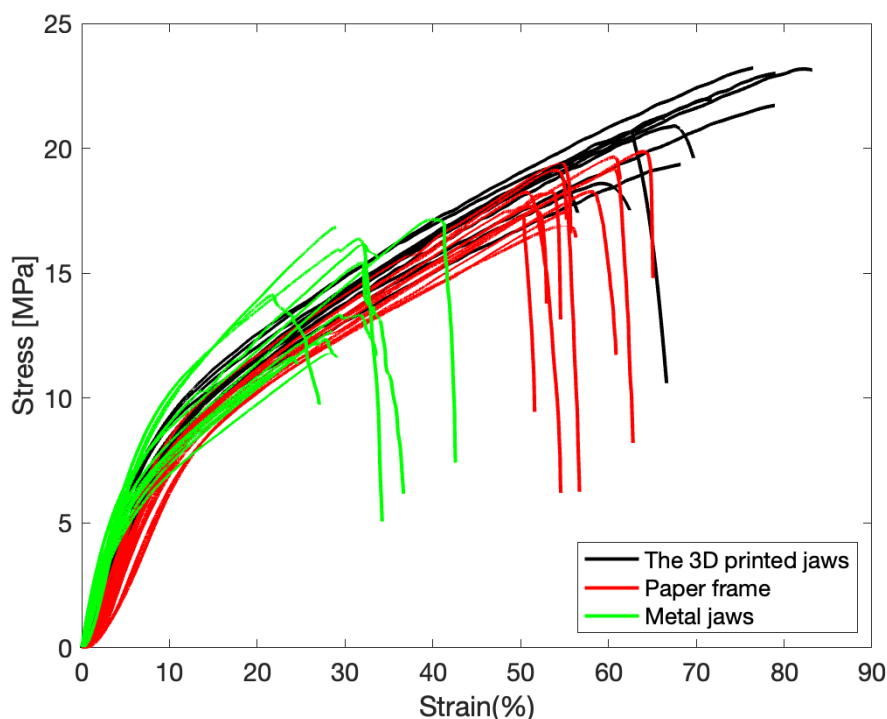


**Figure 4** Comparison of the results of uniaxial tensile tests of an electro-spun membrane with three different clamping systems

The average stress observed for the printed jaws was  $21.0 \pm 2.7$  MPa, whereas the average stress attained via direct positioning between the metal jaws was  $14.1 \pm 5.0$  MPa; the difference was statistically significant ( $p=5.54e-5$ ). The average stress observed for the paper frame was  $18.4 \pm 1.0$  MPa, which was also statistically significant ( $p=1.67e-3$ ) (see Figure 5). Comparison of the results of uniaxial tensile tests of an electro-spun membrane with three different clamping systems

Figure ).

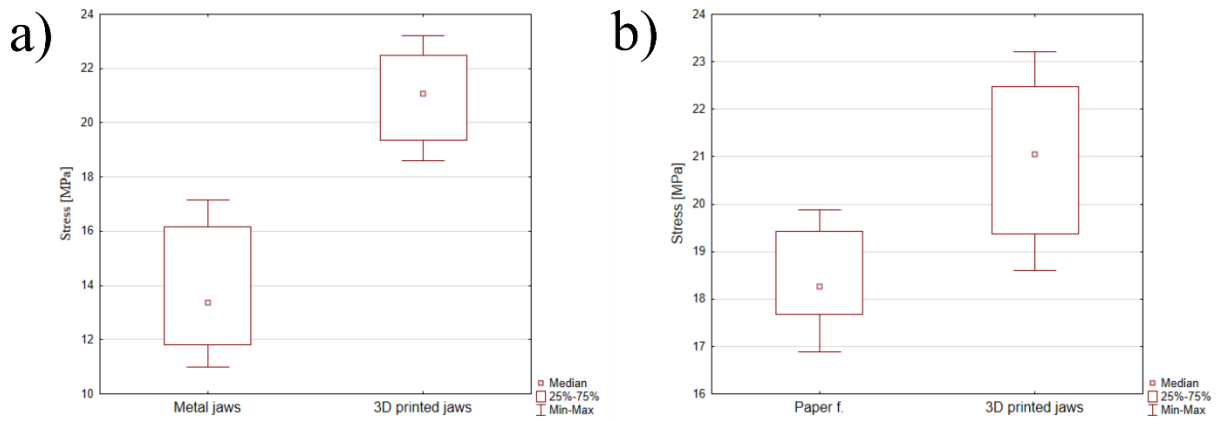


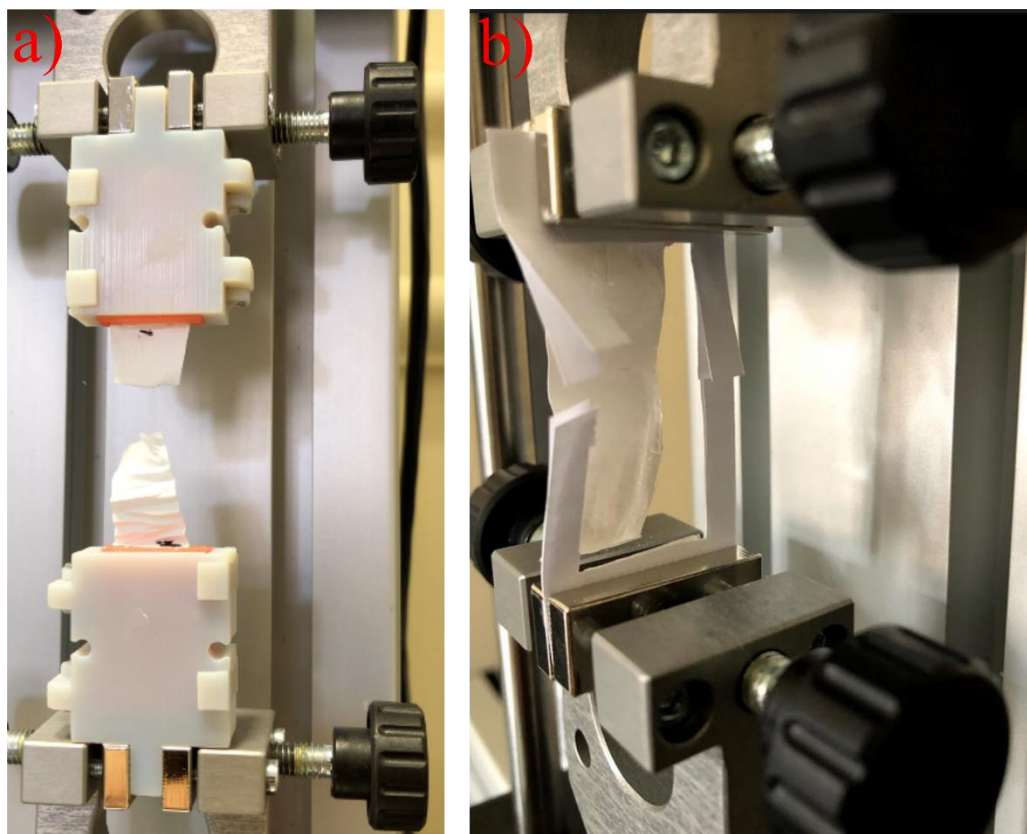
**Figure 5** Comparison of the maximal stress [MPa] for the three clamping systems (upper hatched box = 75th percentile, lower hatched box = 25th percentile) A). Comparison of the maximal stress for the metal jaws and the 3D printed jaws and B) for the paper frame and the 3D printed jaws

**Table 3** shows the average values of the maximal stress and the strain that was attained for the maximal stress. The lowest average force related to the metal jaws due to the fact that the samples were quickly broken by the edges of the metal jaws. An average strain value of 28.85% was attained for the maximal force, while that for the 3D printed jaws was 2.5 higher; moreover, in this case the samples snapped in the middle of the length of the sample (see Figure A).

**Table 3** Comparison of the mean measured ultimate stress and strain values

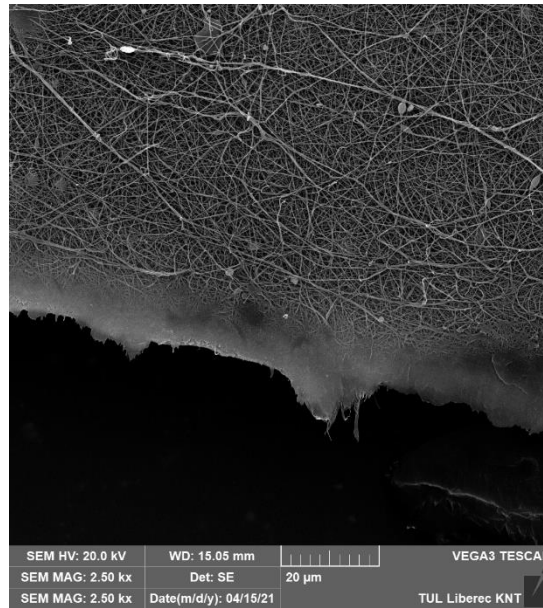
Type of clamping	$\sigma_{avg}$ [MPa]	Strain <sub>avg</sub> [%]
3D printed jaws	21.0 +/- 2.7	68.36 +/- 9.92
Paper frame	18.4 +/- 1.0	55.64 +/- 4.35
Metal jaws	14.1 +/- 5.0	28.85 +/- 5.01

In the case of the paper frame, the average strain value for the maximal **stress** was 1.2 times lower than that of the printed jaws. The **stress** was 1.3 greater and, as with the metal jaws, the samples snapped at the edge of the paper frame (see Figure B).



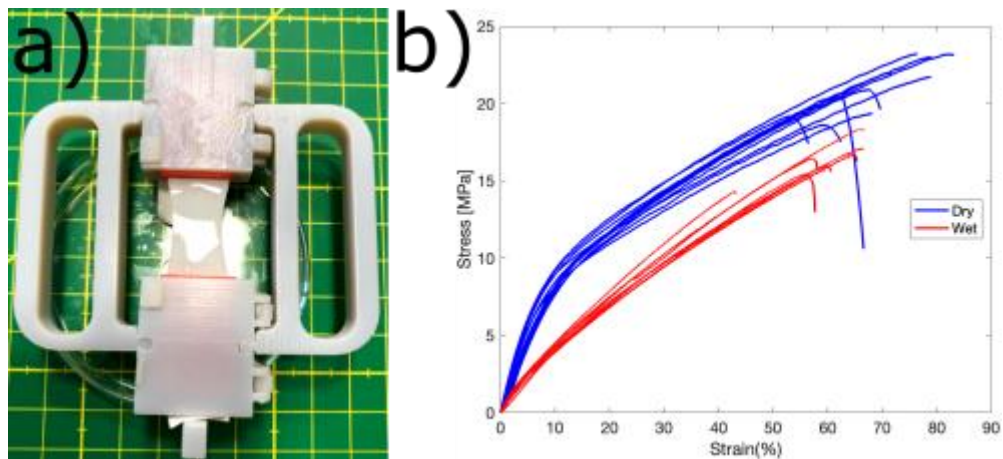
**Figure 6** A) Snapping of the sample in the printed jaws and B) in the paper frame

Figure shows the breaking edge of the sample in the 3D printed jaws. One of the advantages of the printed jaws is their usability for wetted membranes. In case of the metal jaws and the paper frame, the measurements were unfeasible, this was not a case of the printed jaws.



**Figure 7** The breaking edge of the sample analysed by SEM

The membranes were placed in the jaws and wetted by NaCl 0.9% for 10 minutes (see Figure A). The mechanical properties of the electro-spun membranes changed following wetting (see Figure B). The average stress decreased by 4.5 MPa and the average strain at the maximal stress by 9.25%.



**Figure 8** a) Wetting of a membrane using NaCl 0.9%, b) The **stress**-strain curves for the wetted and dry membranes

## Conclusion

Experimentation comprises the golden standard for the establishment of causality, several issues act to undermine the internal validity of experimental findings.<sup>29</sup> This study addresses a **new** clamping mechanism design for the uniaxial tensile testing of electro-spun **PA6** membranes. The aim was to design a mechanism that both speeds up and increases the precision of the sample preparation process prior to uniaxial tensile testing, accompanied by a reduction in the amount of waste. The new clamping mechanism was produced via 3D printing technology combined with the vacuum gravitational casting of the silicon components. The new jaws **were compared** with both a paper frame described in the literature and the direct positioning of samples in the metal jaws of the tensile machine. The metal jaws method was identified as the worst approach following the breakage of the samples at just 28.85 % of the strain. While the second method, a paper frame used according to the literature, evinced better testing results than the metal jaws, this approach also led to early snapping of the samples. The 3D printed jaws evinced the highest average strain values and the maximal **stress** of all the tested methods. Moreover, the time required to position the samples in the printed jaws was two times less than the time required for the paper frame. **Likewise, no paper waste was produced moreover considering the fact that one paper frame with dimensions of 50 x 15 mm weights 0.15 grams. We saved 1.8 grams of paper with respect to the fact that the measurement included only 12 samples. This weight corresponds almost to one paper sheet. In addition, these clamps allow testing wet membranes, which are widely used in liquid filtration process.<sup>30-31</sup> In terms of evaluation of the maximal stress-strain values, some studies propose the principles of the elastic energy theory or probabilistic methods, which can be also considered in future work.<sup>32</sup> 3D printed clamps do not have to be necessarily used in case of flat membranes, by an upgrade they might implemented in testing of tubular scaffold blood vessels<sup>33</sup>.**

## Acknowledgement

This work was supported by the Ministry of Education, Youth and Sports of the Czech Republic and the European Union, European Structural and Investment Funds in the frames of Operational Programme Research, Development and Education, project Hybrid Materials for Hierarchical Structures (HyHi, Reg. No. CZ.02.1.01/0.0/0.0/16\_019/0000843) and by the project of the Specific University Research Grant (Reg. No. 21403) provided by the Ministry of Education, Youth and Sports of the Czech Republic in the year 2020.

## References

1. Xue, J, Wu, T, Dai, Y, Xia, Y. Electrospinning and electrospun nanofibers: Methods, materials, and applications. *Chem Rev* 2019;119:5298-5415.
2. García-Mateos, F, Ruiz-Rosas, R, Rosas, J, Rodríguez-Mirasol, J, Cordero, T. Controlling the composition, morphology, porosity, and surface chemistry of lignin-based electrospun carbon materials. *Front Mater* 2019;6:114.
3. Pavlova, ER, Bagrov, DV, Monakhova, K, Piryazev, A, Sokolova, A, Ivanov, D, Klinov, D. Tuning the properties of electrospun polylactide mats by ethanol treatment. *Mater Des* 2019;181:108061.
4. Şimşek, M. Tuning surface texture of electrospun polycaprolactone fibers: Effects of solvent systems and relative humidity. *J Mater Res* 2020;35:332-342.
5. Ameer, J, Pr, A, Kasoju, N. Strategies to tune electrospun scaffold porosity for effective cell response in tissue engineering. *J Funct Biomat* 2019;10:30.
6. Yin, Y, Zhao, X, Xiong, J. Modeling Analysis of Silk Fibroin/Poly ( $\epsilon$ -caprolactone) Nanofibrous Membrane under Uniaxial Tension. *Nanomat* 2019;9:1149.
7. Khoo, W, Chung, S, Lim, S, Low, C, Shapiro, J, Koh, C. Fracture behavior of multilayer fibrous scaffolds featuring microstructural gradients. *Mater Des* 2019;184:108184.
8. Sood, R, Cavaliere, S, Jones, D, Rozière, J. Electrospun nanofibre composite polymer electrolyte fuel cell and electrolysis membranes. *Nano Energy* 2016;26:729-745.

9. Zhang, Y, Ouyang, H, Lim, Ch, Ramakrishna, S, Huang, Z. Electrospinning of gelatin fibers and gelatin/PCL composite fibrous scaffolds. *J Biomed Mater Res B Appl Biomater* 2005;72:156-165.
10. Nasajpour, A, Ansari, S, Rinoldi, Ch, et al. A multifunctional polymeric periodontal membrane with osteogenic and antibacterial characteristics. *Adv Func Mater* 2018;28:1703437.
11. Mckenna, K, Hinds, M, Sarao, R, et al. Mechanical property characterization of electrospun recombinant human tropoelastin for vascular graft biomaterials. *Acta Biomater* 2012;8:225-233.
12. Yano, T, Higaki, Y, Tao, D, et al. Orientation of poly (vinyl alcohol) nanofiber and crystallites in non-woven electrospun nanofiber mats under uniaxial stretching. *Polymer* 2012;53:4702-4708.
13. Kumar, P, Vasita, R. Understanding the relation between structural and mechanical properties of electrospun fiber mesh through uniaxial tensile testing. *J Appl Polym Sci* 2017;134:1-11.
14. Elele, E, Shen, Y, Tang, J, Lei, Q, Khusid, B, Tkacik, G, Carbrelo, C. Mechanical properties of polymeric microfiltration membranes. *J Membr Sci* 2019;591:117351.
15. Tarus, B, Fadel, N, Al-Oufy, A, El-Messiry, M. Effect of polymer concentration on the morphology and mechanical characteristics of electrospun cellulose acetate and poly (vinyl chloride) nanofiber mats. *Alex Eng J* 2016;55:2975-2984.
16. D'Amato, A, Bramson, M, Puhl, D, Johnson, J, Corr, D, Gilbert, R. Solvent retention in electrospun fibers affects scaffold mechanical properties. *Electrospinning* 2018;2:15-28.
17. Liu, D, Li, S, Yang, Y, Jiang, L. Fabrication, mechanical properties and failure mechanism of random and aligned nanofiber membrane with different parameters. *Nanotechnol Rev* 2019;8(1): 218-226.
18. Yao, C, Li, X, Neoh, K, Shi, Z, Kang, E. Surface modification and antibacterial activity of electrospun polyurethane fibrous membranes with quaternary ammonium moieties. *J Membr Sci* 2008;320:259-267.
19. Zhao, Z, Li, J, Yuan, X, Li, X, Zhang, Y, Sheng, J. Preparation and properties of electrospun poly(vinylidene fluoride) membranes. *J Appl Polym Sci* 2005;97: 466-474.
20. Feng, Y, Xiong, T, Jiang, S, Liu, S, Hou, H. Mechanical properties and chemical resistance of electrospun polyterafluoroethylene fibres. *RSC Advances* 2016;6:24250-24256.



21. Conte AA, Sun K, Hu X, Beachley VZ. Effects of Fiber Density and Strain Rate on the Mechanical Properties of Electrospun Polycaprolactone Nanofiber Mats. *Front Chem* 2020;21(8):610.
22. Maksimcuka, J, Obata, A, Sampson, W, et al. X-ray tomographic imaging of tensile deformation modes of electrospun biodegradable polyester fibers. *Front Mater* 2017;4:43.
23. Scholze, M, Singh, A, Lozano, P, Ondruschka, B, Ramezani, M, Werner, M, Hammer, N. Utilization of 3D printing technology to facilitate and standardize soft tissue testing. *Sci Rep* 2018;8:1-13.
24. Scholze, M, et al. Standardized tensile testing of soft tissue using a 3D printed clamping system. *HardwareX* 2020;8: e00159.
25. Rasband, W, ImageJ, U. S. National Institutes of Health, Bethesda, Maryland, USA, <https://imagej.nih.gov/ij/>, 1997-2018.
26. Yan J, Qiang L, Gao Y, Cui X, Zhou H, Zhong S, Wang Q, Wang H. Effect of fiber alignment in electrospun scaffolds on keratocytes and corneal epithelial cells behavior. *J Biomed Mater Res A*. 2012;100(2):527-35.
27. Han, H J, Hong, H, Park S, Kim, D W. Metal–Electrolyte Solution Dual-Mode Electrospinning Process for In Situ Fabrication of Electrospun Bilayer Membrane. *Adv Mater Interfaces* 2020;7: 2000571.
28. Xiang, C, Frey, M W. Increasing mechanical properties of 2-D-structured electrospun nylon 6 non-woven fiber mats. *Materials* 2016;9(4):270.
29. Lonati, S, Quiroga, B, Zehnder, Ch, Antonakis, J. On doing relevant and rigorous experiments: Review and recommendations. *J Oper Manage* 2018;64:19-40.
30. Huang, L, Manickam, SS, McCutcheon, J. Increasing strength of electrospun nanofiber membranes for water filtration using solvent vapor. *J Membr Sci* 2013;436:213-220.
31. Homaeigohar, SS, Buhr, K, Ebert, K. Polyethersulfone electrospun nanofibrous composite membrane for liquid filtration. *J Membr Sci* 2010;365(1-2):68-77.
32. Rahnev, I . Probabilistic localization of the yield point into the rheogram of the textile thread. In: Proceedings of the 15th AUTEX world textile conference, Bucharest, 10–12 June 2015.
33. Soffer, L., et al. (2008). Silk-based electrospun tubular scaffolds for tissue-engineered vascular grafts. *Journal of Biomaterials Science, Polymer Edition*, 19(5), 653-664.

## Figures

Figure 2 a) 3D CAD model of the assembly, the subassemblies are closed b) Detailed view of the opened subassembly c) The printed jaws with opened subassemblies

Figure 2 Distribution of contact pressure within the silicon jaws [MPa]

Figure 3 a) A sample positioned in the jaws, b) A sample positioned in the tensile machine, c) distribution of fibre diameter

Figure 4 Comparison of the results of uniaxial tensile tests of an electro-spun membrane with three different clamping systems

Figure 5 Comparison of the maximal stress [MPa] for the three clamping systems (upper hatched box = 75th percentile, lower hatched box = 25th percentile) A) Comparison of the maximal stress for the metal jaws and the 3D printed jaws and B) for the paper frame and the 3D printed jaws

Figure 6 A) Snapping of the sample in the printed jaws and B) in the paper frame

Figure 7 The breaking edge of the sample analysed by SEM

Figure 8 A) Wetting of a membrane using NaCl 0.9% B) The stress-strain curves for the wetted and dry membranes

## Tables

Table 1 List of selected approaches for tensile testing of electro-spun membranes

Table 2 Chemical composition of VeroGray

**Table 3** Comparison of the mean measured ultimate stress and strain values